MIXED GAUSSIAN-IMPULSE NOISE IMAGE RESTORATION VIA TOTAL VARIATION

P. Rodríguez, R. Rojas

Department of Electrical Engineering
Pontificia Universidad Católica del Perú
Lima, Peru

B. Wohlberg

T5: Applied Mathematics and Plasma Physics
Los Alamos National Laboratory
Los Alamos, NM, USA

ABSTRACT

Several Total Variation (TV) regularization methods have recently been proposed to address denoising under mixed Gaussian and impulse noise. While achieving high-quality denoising results, these new methods are based on complicated cost functionals that are difficult to optimize, which affects their computational performance.

In this paper we propose a simple cost functional consisting of a TV regularization term and ℓ_2 and ℓ_1 data fidelity terms, for Gaussian and impulse noise respectively, with local regularization parameters selected by an impulse noise detector. The computational performance of the proposed algorithm greatly exceeds that of the state of the art algorithms within the TV framework, and its reconstruction quality performance is competitive for high noise levels, for both grayscale and vector-valued images.

Index Terms— Image Restoration, Total Variation, Gaussian noise, Impulse noise

1. INTRODUCTION

Acquired digital images are frequently subject to additive Gaussian noise [1, Ch. 7]; if we then add the degradation due to transmission errors, the observed image will be corrupted by Gaussian with salt-and-pepper (constant value impulse) noise or random-value impulse noise. Given $\mathbf{u}^*$ and $\mathbf{b}$, the original and observed images respectively, then the mixed Gaussian and impulse noise model is summarized by

$$\begin{aligned} \mathbf{v} &= \mathbf{u}^* + \boldsymbol{\eta} \\ b(k) &= \begin{cases} r(k), & \text{with probability } p \\ v(k), & \text{with probability } 1-p \end{cases} \end{aligned} \tag{1}$$

where $\mathbf{u}^*$ corrupted by additive Gaussian noise is written as $\mathbf{v}$, the additive noise $\boldsymbol{\eta}$ is assumed to be a zero mean Gaussian random variable ($\mu_\eta = 0$) with unknown variance σ_η^2, and $b(k)$ represents the elements of $\mathbf{b}$. $r(k)$ is either the salt-and-pepper noise or the random value impulse noise; for the former case, $r(k) = \mathrm{c}_{\min}$ or $r(k) = \mathrm{c}_{max}$ with probability p_1 and p_2 respectively ($p = p_1 + p_2$) and for the latter case $r(k)$ is drawn with a uniform distribution in $[\mathrm{c}_{\min}, \mathrm{c}_{\max}]$

A number of algorithms, some of which are based on TV regularization, have recently been proposed for denoising of images subject to this mixed noise model [2, 3, 4, 5, 6]. The key idea of the methods not based on TV regularization is to use a two-phase approach: detect the outlier pixels before proceeding with the filtering phase. For example, [2] introduced an universal noise removal filter that first detect the impulse corrupted pixels, and estimates its local statistics and incorporate them into the bilateral filter [7], resulting in the trilateral filter. In [5] somewhat similar ideas where used to develop a similarity principle which in turn drives the weights of the "mixed noise filter"; the reconstruction performance (as reported in [5]) outperforms the trilateral filter.

Within the TV framework, most of the algorithms also have an outlier detection pre-processing phase followed by a denoising phase. The approach in [3] is based on two augmented cost functionals ([3, eqs. (15)-(16)]) which have to be chosen depending on the noise characteristics; the reconstruction performance is competitive, but its computational performance is extremely poor. In [4] the computational performance of [3] is improved, although it still is highly dependent on the noise level, specially for high noise levels; In [6] an ℓ^1-ℓ^0 minimization approach was proposed, resulting in a three-phase algorithm; reconstruction quality results and computational performance are quite good when compared with published works (and could be considered state-of-the-art), but the proposed cost functional ([6, eq. (5)]) is complicated and has several regularization parameters which have to be hand-picked, and the use of of a dictionary learning second phase affects the overall computational performance. Finally we mention that [3, 4] only applies to grayscale images whereas [6] also applies to color images.

In this paper we propose a simple cost functional to denoise images corrupted with the mixed noise model. It is computationally efficient, and gives competitive reconstruction quality, particularly for high noise levels, for both grayscale and color images. The outline of the paper is as follows: in Section 2 we give a brief description of the methods used to develop the proposed algorithm. In Section 3 we present our proposed algorithm that is based on the Iterative Reweighted Norm (IRN) algorithm [8] and its extensions

[9, 10, 11]; in Section 4 we provide our computational results where we compare our propose algorithm with [4, 6]; finally in Section 5 we give our concluding remarks.

2. PRELIMINARIES

The standard ℓ^2-TV regularized solution of the inverse problem involving the observed image data $\mathbf{b}$ is the minimum of the functional

$$T(\mathbf{u}) = \frac{1}{p}\left\|\mathbf{u}-\mathbf{b}\right\|_p^p + \frac{\lambda}{q}\left\|\sqrt{\sum_{n\in C}(D_x\mathbf{u}_n)^2+(D_y\mathbf{u}_n)^2}\right\|_q^q, \tag{2}$$

with $C=\{1\}$ (i.e. grayscale images) $p=2$ and $q=1$, as described in [12]. The fidelity term $F_p(\mathbf{u}) = \frac{1}{p}\|\mathbf{u}-\mathbf{b}\|_p^p$ is determined by the noise model (Gaussian for $p=2$) and the regularization term $R_q(\mathbf{u}) = \frac{1}{q}\left\|\sqrt{\sum_{n\in C}(D_x\mathbf{u}_n)^2+(D_y\mathbf{u}_n)^2}\right\|_q^q$ with $q=1$ is the discretization of $|\nabla\mathbf{u}|$, as originally proposed in [12] ($R_q(\mathbf{u})$ is also a valid the discretization of $|\nabla\mathbf{u}|$ for coupled channels). D_x and D_y represent horizontal and vertical discrete derivative operators respectively. It is assumed that 2-dimensional images are represented by 1-dimensional vectors: $\mathbf{u}_n$ ($n\in C$) is a 1-dimensional (column) or 1D vector that represents a 2D grayscale image obtained via any ordering (although the most reasonable choices are row-major or column-major) of the image pixels. Furthermore, for $C=\{1,2,3\}$ (i.e. three-channel color images) we have that $\mathbf{u}=[(\mathbf{u}_1)^T(\mathbf{u}_2)^T(\mathbf{u}_3)^T]^T$ is a 1D (column) vector that represents a 2D color image.

The original TV method has been extended into a more general technique for inverse problems including deblurring, blind deconvolution and inpainting [13]. It has also been extended to handle several noise models, such the salt-and-pepper noise model, the non-homogeneous Poisson noise model and the Speckle (multiplicative) noise model (see among several others [14, 15, 16] respectively).

2.1. IRN approach

The Iteratively Reweighted Norm (IRN) approach was originally developed to restore images corrupted by Gaussian noise or salt-and-pepper noise for grayscale images [8], and then extended to handle vector-valued (e.g. color) images [9] as well as other noise models such the Speckle noise model [10] and the non-homogeneous Poisson noise model [11]. In what follows we provide a brief description of the original IRN algorithm.

The IRN approach represents the ℓ^p and ℓ^q norms in (2) by the equivalent weighted ℓ^2 norms (see [9] for details):

$$T^{(k)}(\mathbf{u}) = \frac{1}{2}\left\|W_F^{(k)^{1/2}}(A\mathbf{u}-\mathbf{b})\right\|_2^2 + \frac{\lambda}{2}\left\|W_R^{(k)^{1/2}}D\mathbf{u}\right\|_2^2 + \zeta \tag{3}$$

where $\mathbf{u}^{(k)}$ is a constant representing the solution of the previous iteration, ζ is a constant value, I_N is a $N\times N$ identity matrix, $\otimes$ is the Kronecker product, $C=\{1\}$, $N=1$ (grayscale) or $C=\{1,2,3\}, N=3$ (vector-valued) and

$$W_F^{(k)} = \operatorname{diag}\left(\tau_{F,\epsilon_F}(A\mathbf{u}^{(k)}-\mathbf{b})\right), \tag{4}$$

$$D = I_N\otimes[Dx^T\,Dy^T]^T \quad W_R^{(k)} = I_{2N}\otimes\Phi^{(k)}, \tag{5}$$

$$\Phi^{(k)} = \operatorname{diag}\left(\tau_{R,\epsilon_R}\left(\sum_{n\in C}(D_x\mathbf{u}_n^{(k)})^2+(D_y\mathbf{u}_n^{(k)})^2\right)\right). \tag{6}$$

The functions

$$\tau_{F,\epsilon_F}(x) = \begin{cases} |x|^{p-2} & \text{if } |x|>\epsilon_F \\ \epsilon_F^{p-2} & \text{if } |x|\le\epsilon_F, \end{cases}, \tag{7}$$

and

$$\tau_{R,\epsilon_R}(x) = \begin{cases} |x|^{(q-2)/2} & \text{if } |x|>\epsilon_R \\ \epsilon_R^{(q-2)/2} & \text{if } |x|\le\epsilon_R, \end{cases} \tag{8}$$

are defined to avoid numerical problems when $p,q<2$ and $A\mathbf{u}^{(k)}-\mathbf{b}$ or $\sum_{n\in C}(D_x\mathbf{u}_n^{(k)})^2+(D_y\mathbf{u}_n^{(k)})^2$ has zero-valued components.

3. PROPOSED ALGORITHM

We will assume that $\mathcal{N}$, the set of outliers (pixels corrupted with impulse noise) is known. For the scope of this paper, the set $\mathcal{N}$ will be estimated either (i) via the adaptive median filter [17] for the salt-and-pepper case, or (ii) via the center weighted median filter [18] for the random value impulse noise case. Using set $\mathcal{N}$ as given information, we propose the cost functional defined by

$$T(\mathbf{u}) = \frac{1}{\lambda_O}\left\|\Lambda\cdot(\mathbf{u}-\mathbf{b})\right\|_1 + \frac{1}{2\lambda_G}\left\|\tilde{\Lambda}\cdot(\mathbf{u}-\mathbf{b})\right\|_2^2 + R_q(\mathbf{u}), \tag{9}$$

for denoising images corrupted with mixed noise, where $\Lambda = \operatorname{diag}(\mathrm{I}_{[\mathbf{u}\in\mathcal{N}]})$, $\tilde{\Lambda} = \mathbf{1}-\Lambda$, $\mathrm{I}_{[.]}$ is the indicator function, $\mathbf{1}$ represents an identity matrix (with the proper dimensions), $R_q(\mathbf{u})$ with $q=1$ is defined as in (2) and λ_O and λ_G are the regularization parameters used on the outliers and Gaussian corrupted pixels respectively.

Defining $\Lambda_O = \operatorname{diag}(1/\lambda_O)*\Lambda$ and similarly $\tilde{\Lambda}_G = \operatorname{diag}(1/\lambda_G)*\tilde{\Lambda}$, then (9) can be written as

$$T(\mathbf{u}) = \left\|\Lambda_O\cdot(\mathbf{u}-\mathbf{b})\right\|_1 + \frac{1}{2}\left\|\Lambda_G\cdot(\mathbf{u}-\mathbf{b})\right\|_2^2 + R_q(\mathbf{u}). \tag{10}$$

Using the same idea as for the IRN algorithm (see Section 2.1), we can replace the ℓ^1-norm term in (10) by a properly weighted ℓ^2-norm and combine the two resulting ℓ^2-norm terms into one:

$$T^{(k)}(\mathbf{u}) \;=\; \frac{1}{2}\left\|W_F^{(k)^{-1/2}}\cdot(\mathbf{u}-\mathbf{b})\right\|_2^2 + R_q(\mathbf{u}), \tag{11}$$

where $W_F = \Lambda_G + {\Omega_F^{(k)}}^{-1/2}\Lambda_O$, and ${\Omega_F^{(k)}}^{-1/2}$ is a diagonal weighting matrix defined as in (4); here we stress that Λ_O and Λ_G induce a partition on the set of pixels. It is interesting to notice that (11) resembles the original TV problem, except in the form of the weighting matrix ${W_F^{(k)}}^{-1/2}$. Furthermore, for a given weighting matrix, (11) can be easily solved since the regularization term can also be approximated by a quadratic term, as for the IRN algorithm. The final solution is computed iteratively.

4. EXPERIMENTAL RESULTS

We compare our propose algorithm with two state of the art methods: CCN (Cai-Chan-Nikolova, [4]) and XZYN (Xia-Zeng-Yu-and-Ng, [6]). We use the peak signal-to-noise ratio PSNR = $10\log_{10}\frac{\mathrm{N}(\max\{\mathbf{u}^*\})^2}{\|\mathbf{u}-\mathbf{u}^*\|_2^2}$ as one of the reconstruction quality metrics to match the results presented in [4, 6]; we also provide the SNR and SSIM [19] metrics whenever possible.

Due to space constraints we only present results for the grayscale, 512×512 pixel, Lena image for Gaussian with salt-and-pepper noise case and for the Gaussian with random value impulse noise case, although results for several other images and cases may also be generated using the the NUMIPAD (v. 0.30) distribution [20], an implementation of IRN and related algorithms. All simulations have been carried out using the above mentioned Matlab-only (version R2009b) code on a 1.73GHz Intel core i7 CPU laptop (L2: 6144K, RAM: 6G); this software/hardware setup is comparable with that used in [6], allowing us to compare the time performance of our algorithm with those presented in [6].

Image	Noise		SNR	PSNR			SSIM	Time (s.)		
	σ	p	Ours	[6]$^{(*)}$	[4]$^{(*)}$	Ours	Ours	[6]$^{(*)}$	[4]$^{(*)}$	Ours
Lena	$\frac{5}{255}$	0.3	20.11	36.20	34.15	34.64	0.89	338	93	34.5
		0.5	18.21	33.93	32.30	32.75	0.87	–	–	34.4
		0.7	15.66	30.76	29.73	30.20	0.83	247	119	26.9
	$\frac{10}{255}$	0.3	17.82	33.19	31.33	32.36	0.83	–	–	36.4
		0.5	16.61	31.51	29.88	31.14	0.81	–	–	35.2
		0.7	14.54	28.98	27.75	29.07	0.78	–	–	30.1
	$\frac{15}{255}$	0.3	16.03	31.49	29.67	30.56	0.76	215	143	32.8
		0.5	15.27	29.95	28.42	29.80	0.75	–	–	38.8
		0.7	13.80	27.53	26,46	28.33	0.74	176	248	41.8

Table 1. Experimental results for the Gaussian (σ) with salt-and-pepper (p) noise case for the Lena (512×512 grayscale) image. $^{(*)}$ Results taken from [6, Tables 7 and 10].

In Tables 1 and 2 we summarize the results for the Gaussian with salt-and-pepper and Gaussian with random value impulse noise cases respectively. The computational performance of our proposed algorithm is almost independent of the noise level and/or mixture kind; this is not the case for the CNN and XZYN algorithms. Moreover our computational performance is twice as fast as that of CNN, and an order of magnitude faster than XZYN for several cases. However, for the Gaussian with salt-and-pepper noise case our reconstruction quality results are, on average, about 1dB (PSNR) lower than XZYN (even though they are slightly better than CCN); similarly for the Gaussian with random value impulse noise case our reconstruction quality results are on average 1 dB and 2 dB (PSNR) below of those reported by CCN and XZYN respectively.

Since our proposed algorithm can be applied to vector-valued images we present a color reconstruction example: in Figure 1 we show two corrupted Lena (512×512) images: Gaussian ($\sigma = 15/255$) with salt-and-pepper ($p = 0.7$) noise and Gaussian ($\sigma = 15/255$) with random-value impulse ($p = 0.3$) noise and their restored versions.

Image	Noise		SNR	PSNR			SSIM	Time (s.)
	σ	p	ours	[6]$^{(*)}$	[4]$^{(*)}$	Ours	Ours	Ours
Lena	$\frac{5}{255}$	0.1	18.28	34.98	33.78	32.81	0.85	34.8
		0.2	16.54	33.64	32.37	31.07	0.80	33.5
		0.3	14.90	32.04	31.21	29.43	0.75	34.9
	$\frac{10}{255}$	0.1	16.66	32.75	31.01	31.19	0.79	32.6
		0.2	15.17	31.66	30.33	29.70	0.73	29.7
		0.3	13.55	30.42	29.42	28.08	0.66	32.0
	$\frac{15}{255}$	0.1	15.31	30.85	29.34	29.84	0.73	35.8
		0.2	13.90	29.98	28.78	28.43	0.67	33.5
		0.3	12.35	29.11	28.20	26.88	0.60	35.1

Table 2. Experimental results for the Gaussian (σ) with random value impulse (p) noise case for the Lena (512×512 grayscale) image. $^{(*)}$ Results taken from [6, Table 8].

5. CONCLUSIONS

We have proposed a simple yet effective TV cost functional for image restoration under mixed Gaussian and impulse noise. The computational performance of the proposed algorithm greatly exceeds that of the state of the art algorithms [4, 6], being an order of magnitude faster for several cases. There is, however, a trade-off to be made for the superior computational performance: for the Gaussian with salt-and-pepper noise case our reconstruction quality results are slightly better than [4], but slightly worse than [6], and for the Gaussian with random value impulse noise case our reconstruction quality results are somewhat worse than those reported by both [4] and [6].

As part of our on-going work, we highlight that our reconstruction quality results could be improved by means of a spatially (and automatic) adaptation scheme for the regularization parameters, such the one used in [11].

6. REFERENCES

[1] A. C. Bovik, *The Essential Guide to Image Processing*, Academic Press, 2009.

[2] R. Garnett, T. Huegerich, C. Chui, and W. He, "A universal noise removal algorithm with an impulse detector," *IEEE Trans. Image Process.*, vol. 14, pp. 1747–1754, 2005.

[3] J. Cai, R. Chan, and M. Nikolova, "Two-phase methods for deblurring images corrupted by impulse plus gaussian noise," *Inv. Prob. Imaging*, vol. 2, no. 2, pp. 187–204, 2008.

[4] J. Cai, R. Chan, and M. Nikolova, "Fast two-phase image deblurring under impulse noise," *J. Math. Imaging Vis.*, vol. 36, pp. 46–53, January 2010.

[5] B. Li, Q. Liu, J. Xu, and X. Luo, "A new method for removing mixed noises," *Sci. China Inf. Sciences*, vol. 54, pp. 51–59, 2011.

[6] Y. Xiao, T. Zeng, J. Yu, and M. Ng, "Restoration of images corrupted by mixed gaussian-impulse noise via l1-l0 minimization," *Pattern Recog.*, vol. 44, pp. 1708–1720, Aug. 2011.

[7] C. Tomasi and R. Manduchi, "Bilateral filtering for gray and color images," in *Proc. ICCV*, 1998, pp. 839–846.

[8] P. Rodríguez and B. Wohlberg, "Efficient minimization method for a generalized total variation functional," *IEEE Trans. Image Process.*, vol. 18, no. 2, pp. 322–332, 2009.

[9] P. Rodríguez and B. Wohlberg, "A generalized vector-valued total variation algorithm," in *Proc. ICIP*, Egypt, Nov. 2009, pp. 1309–1312.

[10] P. Rodríguez, "Nonconvex total variation speckled image restoration via nonnegative quadratic programming algorithm," in *Proc. EUSIPCO*, Spain, Aug. 2011, pp. 288–292.

[11] P. Rodríguez, "Total variation regularization for poisson vector-valued image restoration with a spatially adaptive regularization parameter selection," in *Proc. ISPA*, Croatia, Sep. 2011, pp. 402–407.

[12] L. Rudin, S. J. Osher, and E. Fatemi, "Nonlinear total variation based noise removal algorithms.," *Physica D. Nonlin. Phenomena*, vol. 60, no. 1-4, pp. 259–268, 1992.

[13] T. Chan, S. Esedoglu, F. Park, and A. Yip, "Recent developments in total variation image restoration," in *Hdbk. of Math. Models in Comp. Vis.* Springer, 2005.

[14] M. Nikolova, "Minimizers of cost-functions involving nonsmooth data-fidelity terms. application to the processing of outliers," *SIAM J. Numerical Analysis*, vol. 40, no. 3, pp. 965–994, 2002.

[15] E. Jonsson, S. Huang, and T. Chan, "Total-variation regularization in positron emission tomography," UCLA CAM Report 98-48, 1998, CAM Report 98-48, UCLA.

[16] S. Osher, N. Paragios, L. Rudin, and P. Lions, "Multiplicative denoising and deblurring: Theory and algorithms," in *Geometric Level Set Methods in Imaging, Vision, and Graphics*, pp. 103–119. Springer, 2003.

[17] H. Hwang and Richard A. Haddad, "Adaptive median filters: New algorithms and results," *IEEE Trans. Image Process.*, pp. 499–502, 1995.

[18] S. Ko and Y. Lee, "Center weighted median filters and their applications to image enhancement," *IEEE Trans. Circuits & Syst.*, vol. 38, no. 9, pp. 984–993, 1991.

[19] Z. Wang, A. Bovik, H. Sheikh, and E. Simoncelli, "Perceptual image quality assessment: From error visibility to structural similarity," *IEEE Trans. Image Process.*, vol. 13, no. 4, pp. 600–612, April 2004.

[20] P. Rodríguez and B. Wohlberg, "Numerical methods for inverse problems and adaptive decomposition (NUMIPAD)," `http://numipad.sourceforge.net/`.

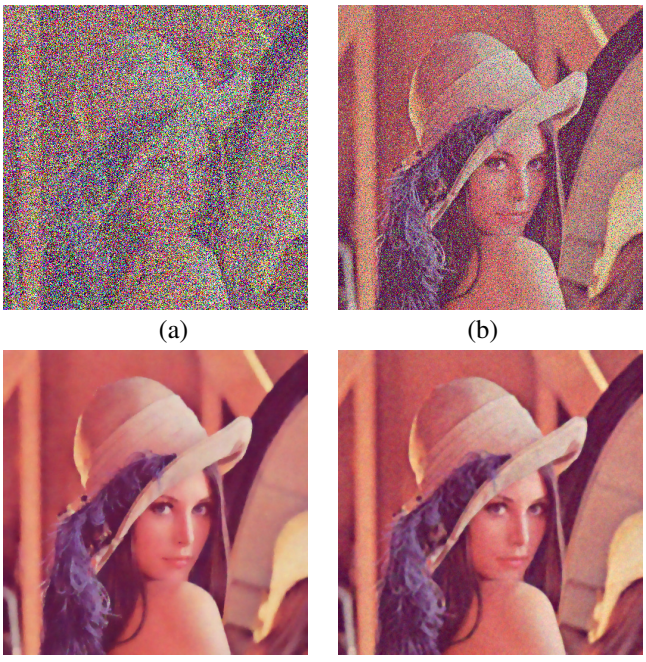

(a) (b) (c) (d)

Fig. 1. Color Lena (512×512) corrupted with (a) Gaussian ($\sigma = 15/255$) with salt-and-pepper ($p = 0.7$) noise, PSNR=6.70 dB and with (b) Gaussian ($\sigma = 15/255$) with random-value impulse ($p = 0.3$) noise, PSNR=13.63 dB; (c) and (d) are the denoised version of (a) and (b) with PSNR equal to 27.82 dB and 26.77 dB respectively.